Biological Psychiatry

Archival Report

Personalized Intrinsic Network Topography Mapping and Functional Connectivity Deficits in Autism Spectrum Disorder

Erin W. Dickie, Stephanie H. Ameis, Saba Shahab, Navona Calarco, Dawn E. Smith, Dayton Miranda, Joseph D. Viviano, and Aristotle N. Voineskos

ABSTRACT

BACKGROUND: Recent advances in techniques using functional magnetic resonance imaging data demonstrate individually specific variation in brain architecture in healthy individuals. To our knowledge, the effects of individually specific variation in complex brain disorders have not been previously reported.

METHODS: We developed a novel approach (Personalized Intrinsic Network Topography, PINT) for localizing individually specific resting-state networks using conventional resting-state functional magnetic resonance imaging scans. Using cross-sectional data from participants with autism spectrum disorder (ASD; n = 393) and typically developing (TD) control participants (n = 496) across 15 sites, we tested: 1) effect of diagnosis and age on the variability of intrinsic network locations and 2) whether prior findings of functional connectivity differences in persons with ASD compared with TD persons remain after PINT application.

RESULTS: We found greater variability in the spatial locations of resting-state networks within individuals with ASD compared with those in TD individuals. For TD persons, variability decreased from childhood into adulthood and increased in late life, following a U-shaped pattern that was not present in those with ASD. Comparison of intrinsic connectivity between groups revealed that the application of PINT decreased the number of hypoconnected regions in ASD.

CONCLUSIONS: Our results provide a new framework for measuring altered brain functioning in neurodevelopmental disorders that may have implications for tracking developmental course, phenotypic heterogeneity, and ultimately treatment response. We underscore the importance of accounting for individual variation in the study of complex brain disorders.

Keywords: Autism spectrum disorder, Child development, Connectome, Functional magnetic resonance imaging, Individuality, Resting state

https://doi.org/10.1016/j.biopsych.2018.02.1174

Disease heterogeneity has been a major obstacle in the study of neurodevelopmental disorders. Autism spectrum disorder (ASD) is a lifelong complex neurodevelopmental disorder affecting 1% of the population (1), and it has been characterized, using neuroimaging, neuropathology, and other investigative techniques, by both hyperconnectivity and hypoconnectivity. Such heterogeneity is often attributed to different disease subtypes, IQ, age range, sex or gender, or treatment effects or magnetic resonance imaging scanner differences. However, variability among individuals is a topic of emerging interest that may have broad implications for our understanding of neurodevelopmental disorders such as ASD and ultimately for guiding approaches to treatment.

Each human being may possess his or her own unique intrinsic neural topography (2). Individually specific topography can be measured reproducibly in healthy individuals using intrinsic connectivity (3–6). These emerging techniques offer a capacity for stronger alignment of functional signals across individuals, which may ultimately enhance the possibility of treatment translation. Within the ASD literature, at the individual level, Hahamy and colleagues (7) found greater spatial variability of interhemispheric connectivity in approximately 80 ASD cases compared with 80 typically developing (TD) controls, raising the question of whether such increased variability exists within specific brain networks. Further, it raises several questions: 1) how does individually specific topography change in atypical versus typical development (i.e., with age), and 2) what does the presence of individually specific topography mean for interpretation of group-based findings in ASD and other neurodevelopmental disorders that are reported in the literature?

To address these questions, we developed an iterative algorithm, Personalized Intrinsic Network Topography (PINT), and made it publicly available. For each participant in a dataset, the PINT algorithm shifts the locations of so-called

SEE COMMENTARY ON PAGE 236

 ISSN: 0006-3223

template regions of interest (ROIs) to a nearby cortical location, or "personalized" ROI, that maximizes the correlation of the ROI with the rest of the ROIs from its network. Here, we applied the PINT algorithm to resting-state functional magnetic resonance imaging (fMRI) data in a large sample from the Autism Brain Imaging Data Exchange I (ABIDE I) dataset (8). We first tested the stability and reliability of intrinsic network identification using PINT in the same participants over time with the longitudinal subsample of the ABIDE I dataset (n = 31, from two sites) as well as additional TD longitudinal samples from the Consortium for Reliability and Reproducibility (n = 202 across three sites) (9). We then proceeded to investigate the following main questions using ABIDE I cross-sectional data from participants with ASD (n = 393) and TD control participants (n = 496) across 15 sites: 1) is variability of intrinsic networks increased in ASD cases compared with TD controls, thus acting as a marker of ASD, 2) what is the effect of age (and potentially neurodevelopment) on intrinsic network variability, and 3) do prior findings of functional connectivity differences in ASD cases versus TD controls remain after PINT application?

METHODS AND MATERIALS

Datasets

We employed the publicly available ABIDE I resting-state dataset (8) of ASD and TD participants from 17 sites. (For details of the scanning parameters for each individual site, see ABIDE I at http://fcon_1000.projects.nitrc.org/indi/abide/abide_I.html). Data from the Oregon Health and Science University site were not included because the shorter duration of the resting-state scans was not suitable for the FMRIB Software Library independent component analysis–based denoising software FIX (see the Preprocessing Pipeline subsection). Data from the Stanford site were excluded because of the poor quality of the anatomical images, leading to a poor performance of our FreeSurfer (https://surfer.nmr.mgh.harvard.edu) pipeline. Demographic criteria from participants included in our analyses (n = 393 ASD cases, n = 496 TD controls, across 15 sites, 6–65 years of age) are described in Supplemental Table S3.

Test–retest performance and longitudinal stability of the PINT algorithm was tested using three datasets of TD individuals obtained from the Consortium for Reliability and Reproducibility (http://fcon_1000.projects.nitrc.org/indi/CoRR/html), of similar age and scan parameters as those of ABIDE I: New York University dataset NYU_2 (https://doi.org/10.15387/fcp_indi.corr.nyu2; 8–55 years of age, n = 187 retested same session, n = 62 with 6 months of follow-up); University of Utah Health Care dataset Utah_1 (https://doi.org/10.15387/fcp_indi.corr.utah1; n = 26, 8–38 years of age, scanned 2 years apart, with a repeated scan in the second session); and University of Pittsburgh School of Medicine dataset UPSM (https://doi.org/10.15387/fcp_indi.corr.upsm1; n = 100, 10–20 years of age, scanned 2 years apart). Additionally, the longitudinal stability of the PINT algorithm was tested in the ABIDE longitudinal sample (http://fcon_1000.projects.nitrc.org/indi/abide/abide_II.html), a release of ASD and TD participants' 2-year follow-up scans from the University of California–Los Angeles (n = 21, 10–13 years of age) and the University of Pittsburgh School of Medicine (n = 17, 9–17 years of age). Scanning parameters and participant demographics are summarized in the Supplement.

Preprocessing Pipeline

Magnetic resonance images were preprocessed using a workflow that is described in the Preprocessing Pipeline section of the Supplement and was adapted from the Human Connectome Project Minimal Processing Pipeline (10) to register data into a combined volume and cortical surface–based analysis format (cifti format in "MNINonLinear-fsaverage_LR32" space). Adapted scripts are available at https://github.com/edickie/ciftify. The cortical surfaces were defined using FreeSurfer's recon-all pipeline (version 5.3). Resting-state scans were preprocessed using a combination of AFNI and FSL tools for despiking, slice timing, motion correction, and independent component analysis–based data-cleaning using FIX. Quality assurance metrics for the resting state scans were assessed using the Quality Assurance Pipeline (https://github.com/preprocessed-connectomes-project/quality-assessment-protocol, accessed July 15, 2016). After scans of low quality were excluded (see Supplemental Methods), quality assurance metrics from the remaining participants were transformed to normality and submitted to a principal component analysis. The top two principal components accounted for a total of 83% of the variance in temporal scan quality (see Supplemental Table S1 for loadings) and were included as covariates in all subsequent analyses.

The PINT Algorithm and Template ROIs

Eighty template vertices were chosen to sample from six resting-state networks described in Yeo *et al.* (11): dorsal attention, default mode (DM), ventral attention (VA), frontoparietal, sensory motor (SM), and visual. The limbic network from the seven-network atlas was not employed because it contains areas of high fMRI signal susceptibility. The locations of the 80 ROIs are given in Supplemental Table S2 and plotted in Figure 1. Average seed correlation maps, shown in Supplemental Figures S1 and S2, strongly resemble the Yeo seven-network atlas. Therefore, we are confident that these 80 template ROIs represent a good sample of network activity. PINT fits an individual participant's resting connectivity matrix to a template pattern of networks by moving the locations for sampling ROIs, iteratively, in a manner that optimizes the within-network connectivity. The code is available at https://github.com/edickie/ciftify; see ciftify_PINT_vertices. During each iteration, for each ROI, PINT calculates the partial correlation of each vertex within a 6-mm search radius of a start vertex, and the other ROIs from the same network, and then moves the ROI's position to the vertex of highest partial correlation (see depiction in Figure 1). Details of the algorithm's performance in the ABIDE I sample are given in the Supplement. An evaluation of PINT as a function of internal algorithm parameters is reported in the Supplement.

Statistical Analyses

Test–retest reliability and longitudinal stability were measured by comparing the distance (measured on the average surface of the Human Connectome Project 900 Subjects release at

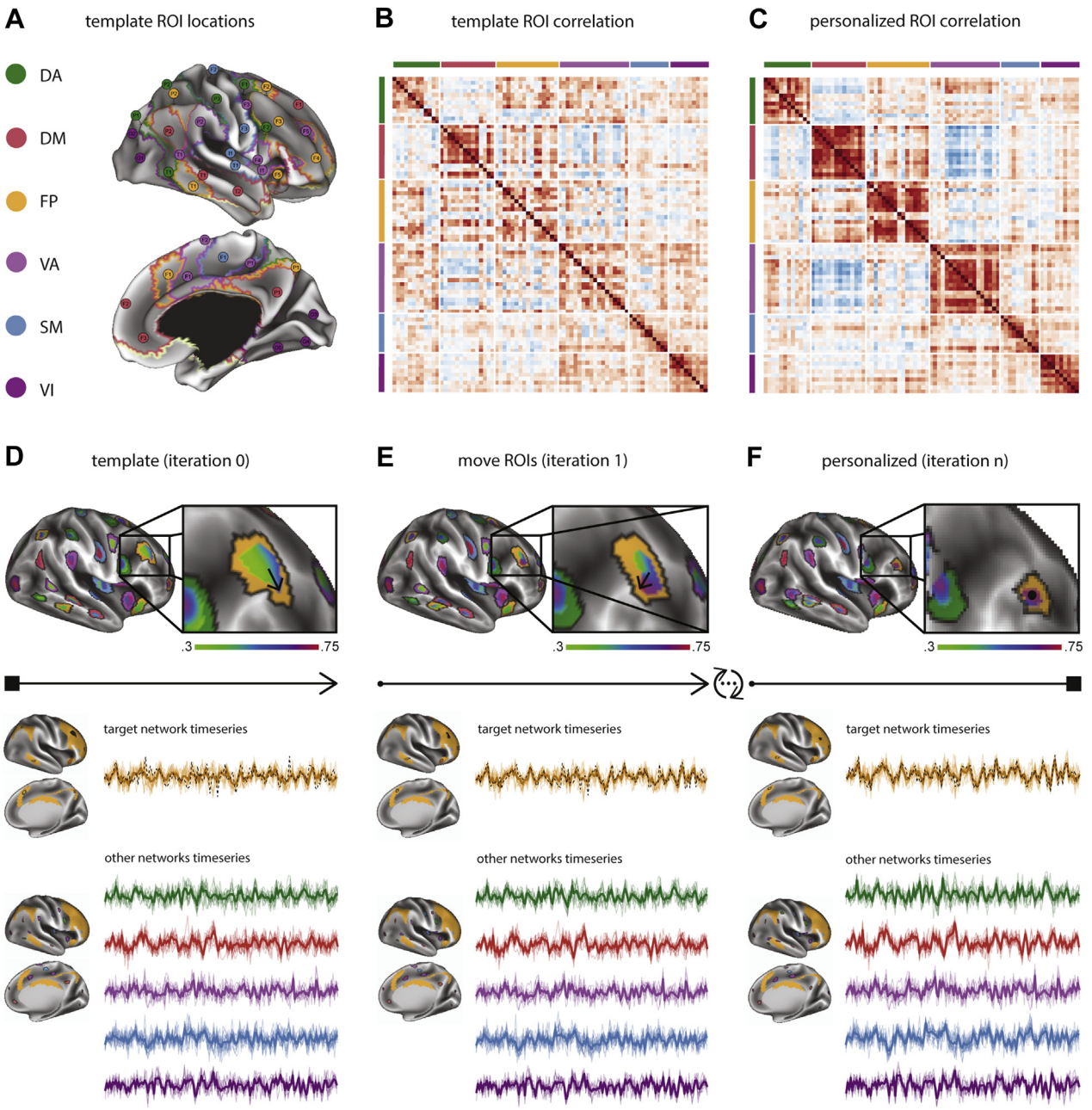

Figure 1. Schematic of the Personalized Intrinsic Network Topography (PINT) method. **(A)** PINT starts with a template set of regions of interest (ROIs) selected from the atlas of Yeo *et al.* (11). **(B)** Template (input) and **(C)** personalized (output) correlation matrices from a representative subject. **(D)** PINT starts by calculating average mean time series from circular ROIs of 6-mm radius around 80 central template vertices. In this depiction, we zoom in on an ROI from the frontoparietal network. The correlation of a vertex time series (dashed black line) is calculated with the frontoparietal network time series (orange line) after the time series of the five other networks are regressed from both. Then, the center of the ROI is moved to the vertex of maximal partial correlation (the direction of movement is show using the black arrow). **(E)** After all 80 ROIs have been moved, the network time series are updated and the algorithm repeats around the new vertex locations. **(F)** The algorithm iterates until all 80 ROIs are centered about a vertex of highest partial correlation (represented by the black circle). DA, dorsal attention network; DM, default mode network; FP, frontoparietal network; SM, sensory motor network; VA, ventral attention network; VI, visual network. (Note: The limbic network was not included, because it contains many areas of high functional magnetic resonance imaging signal susceptibility.)

midsurface) between the baseline and follow-up personalized ROI locations. Within-subject distance was compared with the mean cross-subjects distance via paired *t* tests.

Individual variability in intrinsic network locations was calculated as the distance from the starting template vertex location to each participant's personalized vertex location,

measured on the Average Surface of the Human Connectome Project 900 Subjects release. This distance was averaged across all 80 ROIs for each participant to build a total-brain score and within each network to produce network-level scores. We used linear regression to test for effects of diagnosis and age-by-diagnosis interactions on average distance. All linear models included covariates of age, sex (per ABIDE data dictionary), IQ, site, cortical surface area, and the top two principal components of scan quality metrics. To identify nonlinear age effects, the total-brain score was regressed against the same model with a quadratic age term introduced and the same covariates. To confirm the nature of age effects in those ≤30 years of age, both the nonlinear (quadratic) and linear models were repeated after excluding participants (37 ASD cases, 33 TD controls >30 years of age). Network-level analyses were corrected for multiple comparisons using false discovery rate.

To visualize personalized ROI locations within groups of people, we created vertexwise probability maps. A difference map was created by subtracting the probability map of the ASD cases from that of TD controls. This map was thresholded using permutation tests. We permuted group membership to create 2000 "random" group difference maps. Then, at each vertex, we took difference values between the 2.5th and 97.5th percentiles as our cutoff for significance ($\alpha = .05$, two tailed). A similar process was used to create difference maps between children and young adults.

Edges from Z-transformed correlation matrices calculated from time series of pre-PINT adjustment template ROIs and post-PINT personalized ROIs were tested for a difference between ASD and TD groups, in a linear regression with covariates of age, sex, IQ, scanning site, and the two top principal components of scan quality measures, using linear regression. False discovery rate was used to correct for multiple comparisons. Follow-up analyses, testing for associations of edgewise connectivity with Autism Diagnostic Observation Schedule (ADOS) scores and full-scale IQ values, were conducted using those participants with ASD who had data for these scales using the same covariates (age, sex, site, and the top two principal components of scan quality measures).

The code for all preprocessing and statistical analyses is available at https://bitbucket.org/edickie/abide-pint.

RESULTS

Test–Retest Reliability and Longitudinal Stability of the PINT Algorithm

In all test–retest and longitudinal datasets tested, we found that the distance, measured on the surface, between personalized ROI locations was lower when measured via within-subject method than when measured via the cross-subject method (see Figure 2). Note that the within-subject versus cross-subject distance effects were greater in datasets where both baseline and follow-up scans were acquired on the same day than in those tested months or years apart. This finding supports suggestions that some reorganization of intrinsic connectivity occurs across development (12,13). This within- versus cross-subject difference was significant for all six resting-state networks tested (see Supplemental Figure S9) and irrespective of ASD or TD group membership (see Supplemental Table S7). We also found greater within-subject than cross-subject similarity in the resulting correlation matrices (described in the Supplement and Supplemental Table S8).

Application of PINT Increases Long-Range Within-Network Correlations

The personalized ROI centers were within an average of 7.70 mm of the template vertex locations (see Supplemental Figure S3 for detailed probabilistic maps). Vertex displacement was not correlated with in-scanner head motion (see Supplemental Figure S4). The average ($n = 889$) Z-transformed correlation values are shown in Supplemental Figure S5. Within resting-state network functional connectivity increased substantially across the sample of ASD and TD participants when personalized ROI locations were used (template ROI mean correlation [Z] = 0.34, SD = 0.12; personalized ROI mean = 0.52, SD = 0.13; see Supplemental Table S4). In addition, regional spatial heterogeneity of long-range connectivity was decreased in the personalized ROIs (paired $t_{888} = -22.13$, $p < 10^{-16}$; see Supplemental Figure S6).

Intrinsic Network Locations Are More Variable in ASD Cases Than in TD Controls

We found that individual subject distances to the template ROI center were greater in the ASD group than in the TD group ($t_{867} = 3.05$, $p = .002$). Additional significant predictors to the model included site ($F_{14,867} = 14.3$, $p < .001$), participants' total surface area ($t_{867} = -4.73$, $p < .001$), and (marginally) the first principal component of temporal scan quality metrics ($t_{867} = 1.92$, $p = .06$).

Intrinsic Network Location Variability Follows a U-Shaped Curve Pattern Across the Lifespan in the TD Group, but Shows No Relationship With Age in the ASD Group

Within the TD group, the mean distance from the template ROI center to personalized ROI center (across the 80 ROIs tested) was negatively associated with age ($t_{475} = -3.17$, $p = .002$). Under further exploration, the effect of age in the TD group was best described by a quadratic curve, where the total distance decreased from childhood to adulthood but then increased again after 30 years of age (see Supplemental Figure S7) (quadratic term $t_{474} = 3.07$, $p = .002$). If only those TD participants aged 30 and below are included, the age effect is best modeled as a linear decline ($t_{442} = -4.26$, $p = .000025$). Individuals with ASD showed no such age effect: neither a linear decline ($t_{371} = -1.49$, $p = .14$) nor quadratic curve ($t_{371} = 0.31$, $p = .75$) was observed. However, a significant age-by-diagnosis effect was found ($F_{2,864} = 3.19$, $p = .04$).

Network-Level Analysis of Intrinsic Network Locations

Given the age effects described above in TD participants, we assessed each of the six functional networks separately in participants <30 years of age (see Table 1). We found an effect of diagnosis and a diagnosis-by-age interaction in the VA and dorsal attention networks (see Table 1 and Figure 3A). For the DM network, an effect of age was present (see Table 1). Spatial variability in DM ROIs decreased with age (ASD group:

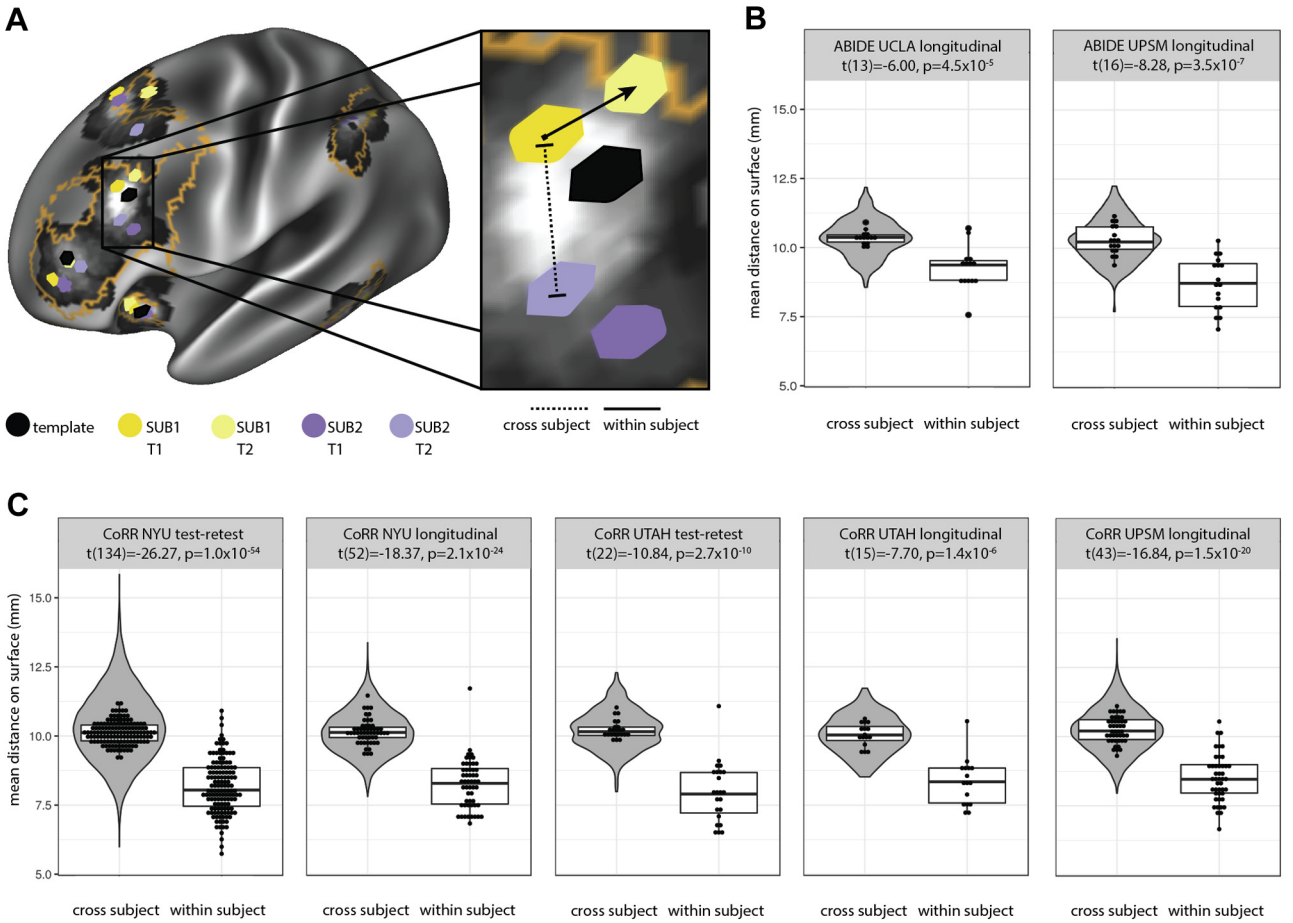

Figure 2. Test–retest and longitudinal stability of Personalized Intrinsic Network Topography (PINT) using Autism Brain Imaging Data Exchange (ABIDE) longitudinal and Consortium for Reliability and Reproducibility (CoRR) datasets. **(A)** Measurement of within-subject and cross-subject distance for a personalized frontoparietal network region of interest is depicted for two representative longitudinal participants. The orange outline represents the frontoparietal network as defined by the atlas of Yeo *et al.* (11). Template vertex locations are shown in black for reference. **(B)** The locations of PINT personalized vertices show consistency over time. Gray violin plots show the distribution of cross-subject distances (averaging across 80 regions of interest) for the University of California–Los Angeles (UCLA) site (left, n = 14) and University of Pittsburgh School of Medicine (UPSM) site (right, n = 17). Box plot and points, for the cross-subject measure, show the mean distance of each individual's baseline scan to all other individuals' follow-up scans. This measure is compared with the distance of each individual's baseline scan to his or her own follow-up scan (within subject distance). **(C)** This effect replicated in test–retest and longitudinal comparisons in three samples of typically developing individuals obtained from the Consortium for Reliability and Reproducibility (left to right): NYU_2 test–retest, n = 135 scanned same session; NYU_2 longitudinal, n = 53 scanned approximately 6 months apart); Utah_1 test retest; n = 23, scanned same session; Utah_2 longitudinal, n = 16, scanned approximately 2 years apart; UPSM longitudinal, n = 44, scanned approximately 2 years apart. NYU, New York University; SUB1 T1, subject 1, time 1; SUB 1 T2, subject 1, time 2; SUB2 T1, subject 2, time 1; SUB2 T2, subject 2, time 2; UTAH, University of Utah School of Medicine.

r = −0.11, p = .05; TD group: r = −.10, p = .03) (Figure 3B). There was no effect of ASD diagnosis. However, an exploratory analysis in individuals with ASD revealed a weak trend for an association between spatial variability in DM ROIs and ASD symptom severity (ADOS scores: t_{247} = 1.71, p = .09 uncorrected).

Application of PINT (i.e., Adjusting Individual Differences in Spatial Location) Decreases the Long-Range Hypoconnectivity Otherwise Observed in ASD

Before PINT correction, 214 edges showed significantly lower correlation strength in the ASD group compared with the TD group (Figure 4A). This finding is in high agreement with previous publications of cortical hypoconnectivity in ASD (8). In contrast, after we adjusted for differences in intrinsic network topography, 80 connections showed lower correlations in ASD versus TD groups, and four connections showed higher correlation in ASD versus TD groups (Figure 4B). This finding provides direct support for our hypothesis that some of the cortical hypoconnectivity previously reported in ASD is a product of greater heterogeneity in the spatial locations of the ROIs in the ASD versus that in the TD group.

Effects of Clinical Scores After PINT Application

ADOS total score was negatively correlated with connectivity between the ventromedial prefrontal cortex ROI of the DM

Table 1. Effects of Age and Autism Spectrum Disorder Diagnosis on Personalized Vertex Locations

Network	Age Effect	Diagnosis Effect	Age-by-Diagnosis Interaction
SM	–	$t = -1.75$, $p = .080$	–
VI	–	–	$t = -1.89$, $p = .060$
DM	$t = -2.87$, $p < .001$[a]	–	–
FP	–	–	–
DA	–	$t = -2.73$, $p = .007$[a]	$t = -2.06$, $p = .040$
VA	–	$t = -2.76$, $p = .006$[a]	$t = -2.02$, $p = .040$
All ROIs	–	$t = -3.23$, $p = .001$	$t = -2.49$, $p = .013$

Additional model covariates: Site, sex, full-scale IQ, total cortical surface area, top two principal components of functional magnetic resonance imaging scan quality. Residual degrees of freedom = 886.

DA, dorsal attention network; DM, default mode network; FP, frontoparietal network; ROI, region of interest; SM, sensory motor network; VA, ventral attention network; VI, visual network.

[a]Significant after false discovery rate correction across 6 networks.

network and the frontal pole ROI of the VA network (ADOS total score: $t = 19.3$, $p = .05$, false discovery rate corrected). Several additional edges connecting the VA and DM networks showed a similar negative correlation at a lower threshold ($p < .001$, uncorrected) (see Supplemental Table S5 and Supplemental Figure S8).

DISCUSSION

We found that the spatial organization of the brain's intrinsic functional networks is more variable in ASD cases compared with that in TD controls, most prominently in the dorsal and VA networks. Application of our novel PINT algorithm to a conventional group-based analysis of functional connectivity resulted in a reevaluation of many of the previously shown findings of "hypoconnectivity" in the ASD literature. Intrinsic network location variability showed a nonlinear U-shaped relationship with age across the lifespan in TD participants, but there was no relationship with age in those with ASD. Our findings provide a new understanding of brain network organization and heterogeneity in people with ASD and TD individuals across the developmental lifespan while reconfiguring our understanding of prior findings in the literature.

Our most important finding was greater variability of spatial organization in cortical resting-state networks in the ASD population than in TD control participants. Greater heterogeneity of cortical organization in ASD has been reported recently in spatial patterns of homotopic connectivity (7), cortical organization (14), and altered functional organization of the motor cortex (15,16). The increased variability in functional organization observed in ASD aligns with the broad clinical and genetic heterogeneity associated with altered neurodevelopmental trajectories (17). Recent data estimate that between 400 and 1000 genes are involved in illness susceptibility in ASD (17), with no one genetic polymorphism predicting >1% of ASD cases (18). In addition, epigenetic markers have also been proposed that contribute to both risk for and heterogeneity within ASD (19,20). The functions of many of these genes appear to converge on molecular pathways for early cortical patterning (21,22). However, in

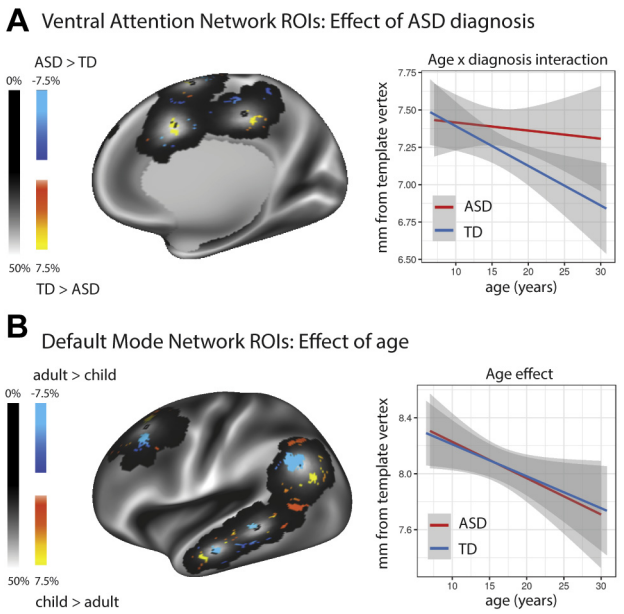

Figure 3. **(A)** Medial right hemisphere view of diagnosis effect on personalized region of interest (ROI) locations in the ventral attention network. The probability map of the personalized ROI location (i.e., one where the value at each vertex represents the proportion of participants in the sample, pooling results from individuals with autism spectrum disorder [ASD] and typically developing [TD] individuals, whose 6-mm ROI encompasses that location) is plotted in grayscale. The template vertex locations are plotted as black dots. The overlaid colors show areas where a significant effect of diagnosis was observed (warm colors, effects in the TD group are greater than effects in the ASD group; cool colors, effects in the ASD group are greater than effects in the TD group). **(B)** Lateral left hemisphere view of age effect on personalized ROI locations in the default mode network. The probability map of the personalized ROI location (all participants ≤30 years of age) is plotted in grayscale. The template vertex locations are plotted as the black dot. The overlaid colors show areas where a significant effect of age group was observed (warm colors: effects in children are greater than effects in adults; cool colors: effects in adults are greater than effects in children). Children were defined as those <12 years of age ($n = 183$); adults were defined as between 18 and 30 years of age, inclusive ($n = 251$).

mouse models, each of the top susceptibility genes for autism has diverse impacts on brain structure (23). Our findings can be interpreted in the context of theories of autism pathology, which posit an early neurodevelopmental insult (22,24–26). It is possible that in the presence of an early neuropathological process, the especially plastic developing brain can maintain the function most critically developing at the time by reappropriating tissue near an area that has become damaged or disconnected. In the case of ASD, with a wide heterogeneity of genetic (27) and environmental influences (28,29) at play, various neuropathological factors could manifest in different cortical locations across individuals (24). A direct consequence could be greater heterogeneity of brain topography.

Group-level differences captured after a functional-based realignment are more likely to reflect "true" disconnect between specific biological targets. In this investigation, after individual differences in network locations were accounted for, within-network connectivity for the SM and DM networks persisted as robust potential neural markers of ASD. Activity within the SM network (8,15,16) as well as connectivity

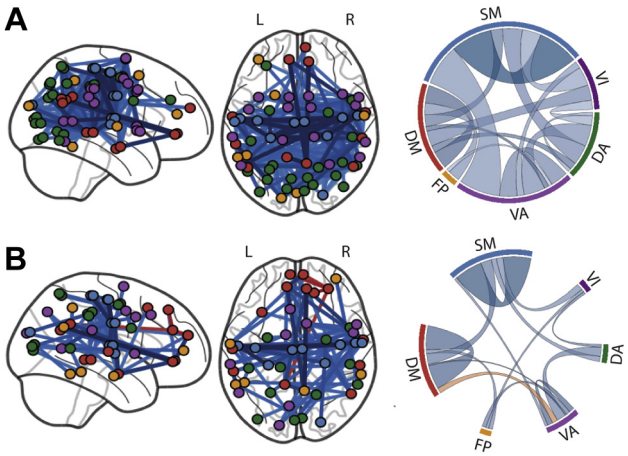

Figure 4. **(A)** Locations (left) and chord diagram of network composition (right) for the 214 edges showing significant hypoconnectivity in autism spectrum disorder calculated from the template regions of interest (before Personalized Intrinsic Network Topography [PINT]). **(B)** After PINT, the number of significant hypoconnected edges (blue) is reduced and four hyperconnected (orange) edges are seen. For the chord diagrams, the width of the chord represents the number of significant edges and the color of the chord represents the mean effect size for those significant edges. DA, dorsal attention network; DM, default mode network; FP, frontoparietal network; L, left; R, right; SM, sensory motor network; VA, ventral attention network; VI, visual network.

between the SM areas and the subcortex (8,30) has been consistently reported in the ASD literature. DM network connectivity decreases have also been frequently reported in the ASD literature (8,31) and have been of great interest because of the proposed role of this network in mentalizing, a core behavioral deficit in ASD (32). Following PINT, four connections between the VA network and the DM network showed newly significant hyperconnectivity in ASD cases compared with that in TD controls. Other connections between the DM network and the VA network were hypoconnected, and they negatively correlated with ASD symptom severity. Given the later maturation of the DM network, it might generally be less susceptible to spatial heterogeneity effects related to ASD or it might not develop more complex relationships such as between-network connectivity to attention network connectivity in ASD; therefore, it requires further exploration.

A key implication of our results is that consideration of increased individual variability among individuals with ASD might be required for future imaging and postmortem brain analysis. It has been previously proposed that some of the hypoconnectivity measured in ASD was not a "true" drop in connection strength between two ROIs but rather attributable to greater heterogeneity across individuals in the locations of the functional areas (7). Our findings confirm this contention on a wide scale (i.e., across brain functional networks), although some networks, namely the dorsal and VA networks, were more susceptible than others. This finding has implications for the emerging view of salience network function as a marker of ASD pathology (33), as the salience network is encompassed by the VA network. Recently, Uddin and colleagues (34) found that maps of the independent component analysis component for the salience network could be used to classify ASD and TD individuals. When we conducted the conventional functional connectivity comparison between ASD and TD participants, while accounting for the PINT correction, the finding of cortical hypoconnectivity with these ROIs in ASD was reduced. Therefore, the mechanism by which the salience network function is affected by ASD is not through disconnection but through idiosyncratic connection.

Our findings also revealed an effect of age, whereby in TD cases, we observed that the distance of individuals' personalized ROI locations from the template vertex location decrease from childhood to adulthood. With increasing age, the organization of resting-state networks look more like the template (or atlas) organization in TD controls. In contrast, variability tends to increase in later life in the TD group, displaying a retrogenesis-like effect. However, the smaller sample size of older adults examined here limits our ability to make strong conclusions in this regard. The age trajectory that we found in TD individuals is similar to those observed for other measures of brain connectivity across development, including white matter volume (12) and white matter microstructure (13,35,36). Critically, recent evidence links these structural changes to the emergence of young adult resting-state network dynamics. Coordinated patterns of cortical thinning in adolescence show spatial correspondence to the location of functional networks (37). Moreover, adolescent changes in white matter microstructure support a greater diversity of functional network dynamics (38). In contrast to the between-subject variability in the spatial domain measured here, within-subject variability in the temporal domain shows the opposite pattern developmentally: temporal variability of electroencephalography, magnetoencephalography, and fMRI time-series increases from childhood to adolescence (39,40) and decreases in late life (41). In our study, the age effects we observed were absent in the ASD population, consistent with an altered neurodevelopmental trajectory.

A recent paper identified 260 functional cortical areas using the multimodal combination of all imaging data from the Human Connectome Project, including 2 hours of resting-state fMRI (4). We argue that 80 ROIs from six networks is a reasonable resolution for analysis given that for some sites, as little as 5 minutes of resting fMRI data are available and some motion during the scan is unavoidable. Future development is required to adapt and validate PINT for additional ROI definitions. We are reassured of the validity of our current approach. given the similarity of results observed across runs in our test–retest and longitudinal samples. This longitudinal retest reliability was observed both for the personalized ROI locations and for the resulting correlation matrices. However, it is possible that ROIs we identify here may actually be multiple subregions belonging to the same one of six larger-scale networks (42) and that these subregions may contribute differently to ASD pathology. It is indeed possible that failing to dynamically switch "states" between these subnetworks such that one subnetwork was evoked more than another may appear as a shift in the larger network's location. The PINT algorithm identifies the center of functional areas of interest. It is possible that some neural markers of ASD pathology may reside not at the center of functional areas but in cortical areas between these centers. These template locations of resting state function were defined from young adult resting-state data

(11). Therefore, it is possible that this template organization of resting-state networks is most applicable to the young adult age range.

The current ABIDE data release has a relatively small number of female participants. This is expected, as more males are affected by ASD. In this analysis, we were underpowered to investigate sex- or gender-based differences in network organization, which may manifest differently in male versus female individuals with ASD (43,44). We were also unable to examine the effects of comorbidity, time of day, or substance abuse because of variability across sites in the nature of the clinical assessment. Additionally, the full-scale IQ range within this population was mostly reflective of individuals with average intelligence (IQ $<$ 80), and while IQ was included as a covariate in all analyses, we were unable to examine specific associations.

Conclusions

We show that the identification of personalized functional network organization is possible using conventional resting-state fMRI scans from multiple scanners. These results are reliable over time, suggesting that they indicate a trait-like marker of brain organization. We provide evidence that the spatial organization of cortical resting-state networks is more variable in people affected by ASD. Furthermore, ASD participants did not demonstrate the age-related decreases in variability observed in TD controls. Finally, our results indicated that many findings of widespread hypoconnectivity in ASD are lost following application of PINT, while other new findings emerge. Taken together, these results underscore the importance of accounting for individual variability in the study of complex brain disorders and provide a window into neurobiological heterogeneity among individuals that may be relevant for treatment innovation.

ACKNOWLEDGMENTS AND DISCLOSURES

ANV and SHA acknowledge support related to the present work from the Canadian Institute for Health Research, Ontario Mental Health Foundation, and Centre for Addiction and Mental Health Foundation. ANV also acknowledges support from the Ontario Ministry of Research and Innovation, the Canadian Foundation for Innovation. Support for ABIDE coordination and data aggregation was partially provided by the National Institute of Mental Health (Grant Nos. K23MH087770, R03MH096321, and BRAINS-RO1MH094639-01), by the Leon Levy Foundation, and by gifts from Joseph P. Healy and the Stavros Niarchos Foundation. Support for ABIDE dataset data collection at each site was provided by the National Institutes of Health (Grant Nos. DC011095, MH084164, and K01MH092288 to Stanford University; Grant Nos. HD55748, KO1MH081191, and MH67924 to the University of Pittsburgh; Grant Nos. K08MH092697, P50MH60450, R01NS34783, R01MH080826, and T32DC008553 to the University of Utah School of Medicine; Grant Nos. K23MH087770, R01HD065282, R01MH081218, R21MH084126-NYU, MH066496, R21MH079871, and U19HD035482 to the University of Michigan; Grant Nos. R00MH091238, R01MH086654, and R01MH096773 to Oregon Health and Science University; Grant No. R01MH081023 to San Diego State University; Grant No. 1R01HD06528001 to the University of California–Los Angeles; Grant No. K01MH071284 to Yale University; and Grant No. R01MH080721 to the California Institute of Technology), Autism Speaks (to the Kennedy Krieger Institute; New York University; Olin Neuropsychiatry Research Center, Institute of Living at Hartford Hospital; University of Michigan; University of Pittsburgh; University of Utah School of Medicine; and Yale University), National Institute of Neurological Disorders and Stroke (Grant No. R01NS048527 to the Kennedy Krieger Institute), Eunice Kennedy Shriver National Institute of Child Health and Human Development (to Yale University, University of California–Los Angeles, and Carnegie Mellon University), the Simons Foundation (to Oregon Health and Science University, Yale University, California Institute of Technology, and Carnegie Mellon University), the Belgian Interuniversity Attraction Poles Grant (Grant No. P6/29 to the University of Leuven), Ben B. and Iris M. Margolis Foundation (to the University of Utah School of Medicine), European Commission (Marie Curie Excellence Grant, Grant No. MEXT-CT-2005-023253 to the Social Brain Lab), Flanders Fund for Scientific Research (Grant Nos. 1841313N, G.0354.06, and G.0758.10 and a postdoctoral grant to the University of Leuven), Hartford Hospital (to the Olin Neuropsychiatry Research Center, Institute of Living at Hartford Hospital), John Merck Scholars Fund (to Yale University), Kyulan Family Foundation (to Trinity University), Michigan Institute for Clinical and Health Research (MICHR Predoctoral Fellowship UL1RR024986 to the University of Michigan), National Children's Hospital (to Trinity University), National Initiative for Brain and Cognition National Cancer Institute Human Cancer Models Initiative (Grant Nos. 056-13-014 and 056-13-017 to the Social Brain Lab), Netherlands Organisation for Scientific Research (Grant Nos. 051.07.003, 452-04-305, and 400-08-089 to the Social Brain Lab), the Netherlands Brain Foundation (Grant No. KS 2010(1)-29 to the Social Brain Lab), National Research Service Award Predoctoral Fellowship (Grant No. F31DC010143 to the University of Utah School of Medicine), Research Council of the University of Leuven (to the University of Leuven), Stanford Institute for Neuro-Innovations and Translational Neurosciences (to Stanford University), Leon Levy Foundation (to New York University), Meath Foundation, Adelaide and Meath Hospital (to Trinity University), Stavros Niarchos Foundation (to New York University), UCLA Autism Center of Excellence (to the University of California–Los Angeles), and University of Utah Multidisciplinary Research Seed Grant (University of Utah School of Medicine). Support for Consortium for Reliability and Reproducibility data collection was provided by National Institutes of Mental Health (Grant No. R01MH080243 to University of Pittsburgh School of Medicine and Grant Nos. K08MH092697 and R01MH080826 to the University of Utah School of Medicine).

We thank Martin Lindquist for his guidance in how to measure reproducibility and Adriana Di Martino for advice about the ABIDE dataset. We also thank all sites and investigators who have worked to share their data through ABIDE and the Consortium for Reliability and Reproducibility.

An earlier draft of this manuscript was posted, as a preprint, at https://www.biorxiv.org/content/early/2017/07/11/161893.

The authors report no biomedical financial interests or potential conflicts of interest.

ARTICLE INFORMATION

From the Kimel Family Translational Imaging Genetics Research Laboratory (EWD, SS, NC, DES, DM, JDV, ANV), the Campbell Family Mental Health Research Institute (EWD, SHA, SS, NC, DES, DM, JDV, ANV), and the Margaret and Wallace McCain Centre for Child, Youth, and Family Mental Health (SHA), The Centre for Addiction and Mental Health and the Department of Psychiatry (SHA, SS, ANV), University of Toronto, and the Centre for Brain and Mental Health (SHA), the Hospital for Sick Children, Toronto, Canada.

Address correspondence to Aristotle N. Voineskos, M.D., Ph.D., Kimel Family Translational Imaging Genetics Research Laboratory, The Centre for Addiction and Mental Health, 250 College Street, Toronto, Ontario M5T 1R8, Canada; E-mail: aristotle.voineskos@camh.ca.

Received Jul 13, 2017; revised Feb 23, 2018; accepted Feb 27, 2018.

Supplementary material cited in this article is available online at https://doi.org/10.1016/j.biopsych.2018.02.1174.

REFERENCES

1. Kim YS, Leventhal BL, Koh Y-J, Fombonne E, Laska E, Lim E-C, *et al.* (2011): Prevalence of autism spectrum disorders in a total population sample. Am J Psychiatry 168:904–912.
2. Mueller S, Wang D, Fox MD, Yeo BTT, Sepulcre J, Sabuncu MR, *et al.* (2013): Individual variability in functional connectivity architecture of the human brain. Neuron 77:586–595.

3. Conroy BR, Singer BD, Guntupalli JS, Ramadge PJ, Haxby JV (2013): Inter-subject alignment of human cortical anatomy using functional connectivity. Neuroimage 81:400–411.
4. Glasser MF, Coalson TS, Robinson EC, Hacker CD, Harwell J, Yacoub E, *et al.* (2016): A multi-modal parcellation of human cerebral cortex. Nature 536:171–178.
5. Wang D, Buckner RL, Fox MD, Holt DJ, Holmes AJ, Stoecklein S, *et al.* (2015): Parcellating cortical functional networks in individuals. Nat Neurosci 18:1853–1860.
6. Robinson EC, Jbabdi S, Glasser MF, Andersson J, Burgess GC, Harms MP, *et al.* (2014): MSM: A new flexible framework for Multimodal Surface Matching. Neuroimage 100:414–426.
7. Hahamy A, Behrmann M, Malach R (2015): The idiosyncratic brain: Distortion of spontaneous connectivity patterns in autism spectrum disorder. Nat Neurosci 18:302–309.
8. Di Martino A, Yan C-G, Li Q, Denio E, Castellanos FX, Alaerts K, *et al.* (2014): The autism brain imaging data exchange: Towards large-scale evaluation of the intrinsic brain architecture in autism. Mol Psychiatry 19:659–667.
9. Zuo X-N, Anderson JS, Bellec P, Birn RM, Biswal BB, Blautzik J, *et al.* (2014): An open science resource for establishing reliability and reproducibility in functional connectomics. Sci Data 1:140049.
10. Glasser MF, Sotiropoulos SN, Wilson JA, Coalson TS, Fischl B, Andersson JL, *et al.* (2013): The minimal preprocessing pipelines for the Human Connectome Project. Neuroimage 80:105–124.
11. Yeo BTT, Krienen FM, Sepulcre J, Sabuncu MR, Lashkari D, Hollinshead M, *et al.* (2011): The organization of the human cerebral cortex estimated by intrinsic functional connectivity. J Neurophysiol 106:1125–1165.
12. Giedd JN, Blumenthal J, Jeffries NO, Castellanos FX, Liu H, Zijdenbos A, *et al.* (1999): Brain development during childhood and adolescence: A longitudinal MRI study. Nat Neurosci 2:861–863.
13. Barnea-Goraly N, Menon V, Eckert M, Tamm L, Bammer R, Karchemskiy A, *et al.* (2005): White matter development during childhood and adolescence: A cross-sectional diffusion tensor imaging study. Cereb Cortex 15:1848–1854.
14. Glerean E, Pan RK, Salmi J, Kujala R, Lahnakoski JM, Roine U, *et al.* (2016): Reorganization of functionally connected brain subnetworks in high-functioning autism. Hum Brain Mapp 37:1066–1079.
15. Nebel MB, Joel SE, Muschelli J, Barber AD, Caffo BS, Pekar JJ, Mostofsky SH (2014): Disruption of functional organization within the primary motor cortex in children with autism. Hum Brain Mapp 35:567–580.
16. Müller R-A, Pierce K, Ambrose JB, Allen G, Courchesne E (2001): Atypical patterns of cerebral motor activation in autism: a functional magnetic resonance study. Biol Psychiatry 49:665–676.
17. Geschwind DH, Levitt P (2007): Autism spectrum disorders: developmental disconnection syndromes. Curr Opin Neurobiol 17:103–111.
18. Berg JM, Geschwind DH (2012): Autism genetics: Searching for specificity and convergence. Genome Biol 13:247.
19. Ladd-Acosta C, Hansen KD, Briem E, Fallin MD, Kaufmann WE, Feinberg AP (2014): Common DNA methylation alterations in multiple brain regions in autism. Mol Psychiatry 19:862–871.
20. Loke YJ, Hannan AJ, Craig JM (2015): The role of epigenetic change in autism spectrum disorders. Front Neurol 6:107.
21. Voineagu I, Wang X, Johnston P, Lowe JK, Tian Y, Horvath S, *et al.* (2011): Transcriptomic analysis of autistic brain reveals convergent molecular pathology. Nature 474:380–384.
22. Parikshak NN, Luo R, Zhang A, Won H, Lowe JK, Chandran V, *et al.* (2013): Integrative functional genomic analyses implicate specific molecular pathways and circuits in autism. Cell 155:1008–1021.
23. Ellegood J, Anagnostou E, Babineau BA, Crawley JN, Lin L, Genestine M, *et al.* (2015): Clustering autism—Using neuroanatomical differences in 26 mouse models to gain insight into the heterogeneity. Mol Psychiatry 20:118–125.
24. Stoner R, Chow ML, Boyle MP, Sunkin SM, Mouton PR, Roy S, *et al.* (2014): Patches of disorganization in the neocortex of children with autism. N Engl J Med 370:1209–1219.
25. Courchesne E, Redcay E, Kennedy DP (2004): The autistic brain: Birth through adulthood. Curr Opin Neurol 17:489–496.
26. Courchesne E, Mouton PR, Calhoun ME, Semendeferi K, Ahrens-Barbeau C, Hallet MJ, *et al.* (2011): Neuron Number and Size in Prefrontal Cortex of Children With Autism. JAMA 306:2001–2010.
27. Geschwind DH (2011): Genetics of autism spectrum disorders. Trends Cogn Sci 15:409–416.
28. Patterson PH (2011): Maternal infection and immune involvement in autism. Trends Mol Med 17:389–394.
29. Careaga M, Murai T, Bauman MD (2017): Maternal immune activation and autism spectrum disorder: From rodents to nonhuman and human primates. Biol Psychiatry 81:391–401.
30. Cerliani L, Mennes M, Thomas RM, Di Martino A, Thioux M, Keysers C (2015): Increased functional connectivity between subcortical and cortical resting-state networks in autism spectrum disorder. JAMA Psychiatry 72:767–777.
31. Di Martino A, Ross K, Uddin LQ, Sklar AB, Castellanos FX, Milham MP (2009): Functional brain correlates of social and nonsocial processes in autism spectrum disorders: an activation likelihood estimation meta-analysis. Biol Psychiatry 65:63–74.
32. Li W, Mai X, Liu C (2014): The default mode network and social understanding of others: What do brain connectivity studies tell us. Front Hum Neurosci 8:74.
33. Uddin LQ, Menon V (2009): The anterior insula in autism: underconnected and under-examined. Neurosci Biobehav Rev 33:1198–1203.
34. Uddin LQ, Supekar K, Lynch CJ, Khouzam A, Phillips J, Feinstein C, *et al.* (2013): Salience network–based classification and prediction of symptom severity in children with autism. JAMA Psychiatry 70:869–879.
35. Ashtari M, Cervellione KL, Hasan KM, Wu J, McIlree C, Kester H, *et al.* (2007): White matter development during late adolescence in healthy males: A cross-sectional diffusion tensor imaging study. Neuroimage 35:501–510.
36. Paus T (2010): Growth of white matter in the adolescent brain: Myelin or axon? Brain Cogn 72:26–35.
37. Sotiras A, Toledo JB, Gur RE, Gur RC, Satterthwaite TD, Davatzikos C (2017): Patterns of coordinated cortical remodeling during adolescence and their associations with functional specialization and evolutionary expansion. Proc Natl Acad Sci U S A 114:3527–3532.
38. Tang E, Giusti C, Baum GL, Gu S, Pollock E, Kahn AE, *et al.* (2017): Developmental increases in white matter network controllability support a growing diversity of brain dynamics. Nat Commun 8:1252.
39. McIntosh AR, Kovacevic N, Itier RJ (2008): Increased brain signal variability accompanies lower behavioral variability in development. PLoS Comput Biol 4:e1000106.
40. Misić B, Mills T, Taylor MJ, McIntosh AR (2010): Brain noise is task dependent and region specific. J Neurophysiol 104:2667–2676.
41. Garrett DD, Kovacevic N, McIntosh AR, Grady CL (2011): The importance of being variable. J Neurosci 31:4496.
42. Braga RM, Buckner RL (2017): Parallel interdigitated distributed networks within the individual estimated by intrinsic functional connectivity. Neuron 95:457–471.e5.
43. Lai M-C, Lerch JP, Floris DL, Ruigrok ANV, Pohl A, Lombardo MV, Baron-Cohen S (2017): Imaging sex/gender and autism in the brain: Etiological implications. J Neurosci Res 95:380–397.
44. Alaerts K, Swinnen SP, Wenderoth N (2016): Sex differences in autism: A resting-state fMRI investigation of functional brain connectivity in males and females. Soc Cogn Affect Neurosci 11:1002–1016.